The Meteoritical Society

Meteoritics & Planetary Science 44, Nr 2, 211–220 (2009)
Abstract available online at http://meteoritics.org

The Cali meteorite fall: A new H/L ordinary chondrite

Josep M. TRIGO-RODRÍGUEZ[1, 2*], Jordi LLORCA[3], Alan E. RUBIN[4], Jeffrey N. GROSSMAN[5], Derek W. G. SEARS[6], Mateo NARANJO[6], Stacy BRETZIUS[6], Mar TAPIA[7], and Marino H. GUARÍN SEPÚLVEDA[8]

[1]Institute of Space Sciences-CSIC. Campus UAB, Facultat de Ciències, Torre C5-p2. Bellaterra, Barcelona 08193, Spain
[2]Institut d'Estudis Espacials de Catalunya (IEEC), Gran Capità 2-4, Ed. Nexus, Barcelona 08034, Spain
[3]Institut de Tècniques Energètiques, Universitat Politècnica de Catalunya (UPC), Barcelona, Spain
[4]Institute of Geophysics and Planetary Physics, University of California, Los Angeles, California 90095–1567, USA
[5]U.S. Geological Survey, Reston, Virginia 20192, USA
[6]Arkansas Center for Space and Planetary Sciences, University of Arkansas, Fayetteville, Arkansas 72701, USA
[7]Institut de Ciències del Mar (CSIC), Barcelona, Spain
[8]Departamento de Ciencias Naturales y Matemáticas, Facultad de Ingeniería, Universidad Javeriana de Cali, Colombia
*Corresponding author. E-mail: trigo@aliga.ieec.uab.es

(Received 27 June 2008; revision accepted 21 September 2008)

Abstract–The fall of the Cali meteorite took place on 6 July 2007 at 16 h 32 ± 1 min local time (21 h 32 ± 1 min UTC). A daylight fireball was witnessed by hundreds of people in the Cauca Valley in Colombia from which 10 meteorite samples with a total mass of 478 g were recovered near 3°24.3′N, 76°30.6′W. The fireball trajectory and radiant have been reconstructed with moderate accuracy. From the computed radiant and from considering various plausible velocities, we obtained a range of orbital solutions that suggest that the Cali progenitor meteoroid probably originated in the main asteroid belt. Based on petrography, mineral chemistry, magnetic susceptibility, thermoluminescence, and bulk chemistry, the Cali meteorite is classified as an H/L4 ordinary chondrite breccia.

INTRODUCTION

The fall of the Cali meteorite occurred in the afternoon of July 6, 2007, at 21 h 33 ± 1 min UTC. A daylight bolide brighter than the Moon was widely observed over Colombia; the bolide traveled from north to south and experienced several fragmentation events along its atmospheric trajectory. Eyewitnesses in several municipalities of the Cauca Valley (from Calima, Cerrito, El Darién, Ginebra, Guacari, La Cumbre, Restrepo, Yotoco, and Yumbo) saw the bolide and heard audible detonations a few minutes later. Many people were alarmed and called the emergency and civil defense telephone numbers within a few minutes of witnessing the bolide. As a consequence of the general alarm, the press quickly dispensed the news about the celestial phenomenon around the country.

Although the object was at first thought to have been lost in the middle of the dense forest of the Cauca Valley, a few minutes after the detonation some meteorites penetrated the roofs of several houses on the outskirts of Cali. The owners of these houses, having been alerted by the news coverage, were quickly able to associate the stones that had impacted their roofs with the bolide event. They reported their findings to the press, which then propagated the news throughout Colombia.

Two astronomical associations of Cali, the Asociación de Astrónomos Aficionados de Cali (ASAFI) and the Escuela de Astronomía de Cali (EAC), contacted the Spanish Meteor and Fireball Network (SPMN) just after the fall to receive instructions on how to collect scientific information about the bolide and to initiate a search for meteorites. In the following days, both astronomical groups joined forces to interview eyewitnesses and search the area where the impacts had been reported (the Mariano Ramos, Ciudad Cordoba, Antonio Narino and Laureano Gómez districts). Two additional fragments were found by these groups on July 14, 2007. Some U.S. meteorite dealers alerted by the news also contributed to the recovery of additional pieces. Most of the pieces were collected a few hours or days after the fall and as a result are completely fresh. In total, 10 samples of the meteorite were found; the total recovered mass being about 478 g (Connolly et al. 2008). The first thin sections were made in Barcelona, Spain, in August 2007 from two meteorite specimens kindly provided by Gustavo Noguera and Yolanda Polanco (EAC). Additional thin sections were made from a 20.5 g type specimen donated to the Smithsonian Institution by Mike Farmer.

Table 1. Visual eyewitnesses interviewed to estimate Cali's bolide trajectory. Data in italics are averaged from the observers listed in the last column. Observations used for obtaining the mean trajectory of the bolide are in bold (see Table 2).

Site	Longitude (°W)	Latitude (°N)	Elevation (m)	Beginning Az, Alt (°)	End Az, Alt (°)	Sound/ duration	Name
Guacarí	**76.334**	**3.768**	**1115**	**270, 60**	**200, 33**	**–**	**J.M. Guzmán and M. Collazos**
Pavas	**76.583**	**3.683**	**1968**	**80, 38**	**155, –**	**Explosion after 30 s**	**A. Chávez and I. M. López**
Tuluá	76.217	4.085	627	200, 24	195, 9		N. Collazos
Vereda Bella Vista	76.65	3.617	1910	*44, 11*	*97, 16*	Sound wave/ 3–5 s	O. Hernández, M. Caicedo, and M. L. García
Vereda Potrerillo	76.567	3.800	1291	*235, 16*	–	Yes	John J. Orozco and F. Orozco
Vereda Riogrande	**76.560**	**3.730**	**1708**	**295, 20**	**–**	**–**	**A. F. López**
Vijes	76.446	3.699	1270	178, 48	184, 22	Explosion after 40 s/ <2 s	H. Vivas
Yotoco	**76.386**	**3.863**	**1380**	***205, 47***	***200, 21***	**Explosion after 1.5 min./2–3 s**	**N.E. Escobar, T. Arce, H. Ceballos, and A. Henao**

TRAJECTORY, RADIANT, AND RANGE OF ORBITS

The ASAFI and EAC were successful in their efforts to obtain a reasonable number of theodolite measurements (see Table 1). The procedures employed are similar to those used in a recent study of a daylight bolide over Spain (Docobo et al. 2007). Initially, we traced the trajectory in the sky from different locations. The locations that yielded consistent trajectories were used to build an average trajectory employing the method of intersecting planes (Ceplecha 1987). An average was then obtained for the different stations and tested by using seismic and meteorite data.

The position of the various observation points geometrically favorable with respect to the path of the fireball enabled its trajectory to be determined with moderate accuracy. In initial interviews, several eyewitnesses in Tuluá reported an almost vertical movement of the bolide, although the exact azimuth of the event is difficult to establish without clear horizon references. Observers in Guacarí, Pavas, and Vereda Riogrande provided the most consistent data on the apparent path of the bolide. Key testimony was obtained from Guacarí because the bolide crossed the sky near the zenith. One report was collected by an eyewitness who observed the bolide from inside a local prison surrounded by high walls. The position of the meteorite strewn field was also used to test the fireball trajectory, although the drift caused by winds during the meteorite's dark flight was not taken into account. The fireball's trajectory as projected on the ground is shown in Fig. 2. The coordinates of the bolide's beginning and ending points are given in Table 2.

From the computed trajectory, we were able to obtain the apparent radiant of the bolide (Table 3). From the reported duration of the bolide, a rough estimate of the observed velocity can be made. Several observers in Vereda Buena Vista and Yotoco who claim to have seen the fireball mentioned that it traversed its complete luminous path in about 3 or 4 s. Because the mean length of the visible trajectory was ~55 km, the average velocity of the bolide would have been in the range $V = 15 \pm 3$ km/s. Although this is a very rough approach, it allows us to define a likely range of orbital elements that fit the observations (Table 4). Almost all the orbital solutions suggest a low-inclination, low-eccentricity orbit with an origin in the main asteroid belt; this is similar to the nine previously reported meteorite falls where accurate determinations of the orbital elements were made (e.g., Trigo-Rodríguez et al. 2006). The extreme solution corresponding to a $V_\infty = 18$ km/s seems to be unlikely because that result places the body moving in an orbit with aphelion situated between Saturn and Uranus.

SEISMIC DATA

We analyzed the data provided by Observatorio Sismológico del Sur Occidente (OSSO) for four seismic stations. Two of the four stations detected a clear signal from the bolide. Both signals are highly monofrequent, very similar to typical explosions detected every day at seismic networks (Fig. 3). Consequently, we interpret such signals as having been produced during the atmospheric breakup of the body. Unfortunately, the number of stations is insufficient to constrain the azimuth of the bolide or reconstruct the trajectory as in previous events (Pujol et al. 2006), but the delay in the reception of these signals from both stations agrees quite well with the computed bolide's trajectory. Two

Fig. 1. The first recovered samples of the Cali chondrite. a) The hole excavated in the roof of Jackelin García's building who was the first to show a meteorite to the press. b, c) Two different views of the meteorite found by J. García, which exhibits fusion crust over about 40% of the samples surface. This piece had a weight of 76.6 grams, and was 7 cm in maximum length. d) The hole left in the roof of Gustavo Noguera's house by the meteorite. e) Noguera with his grandchildren showing the different fragments of the meteorite. f) The different fragments shown in greater detail. Images courtesy of Juan C. Mejía (EAC).

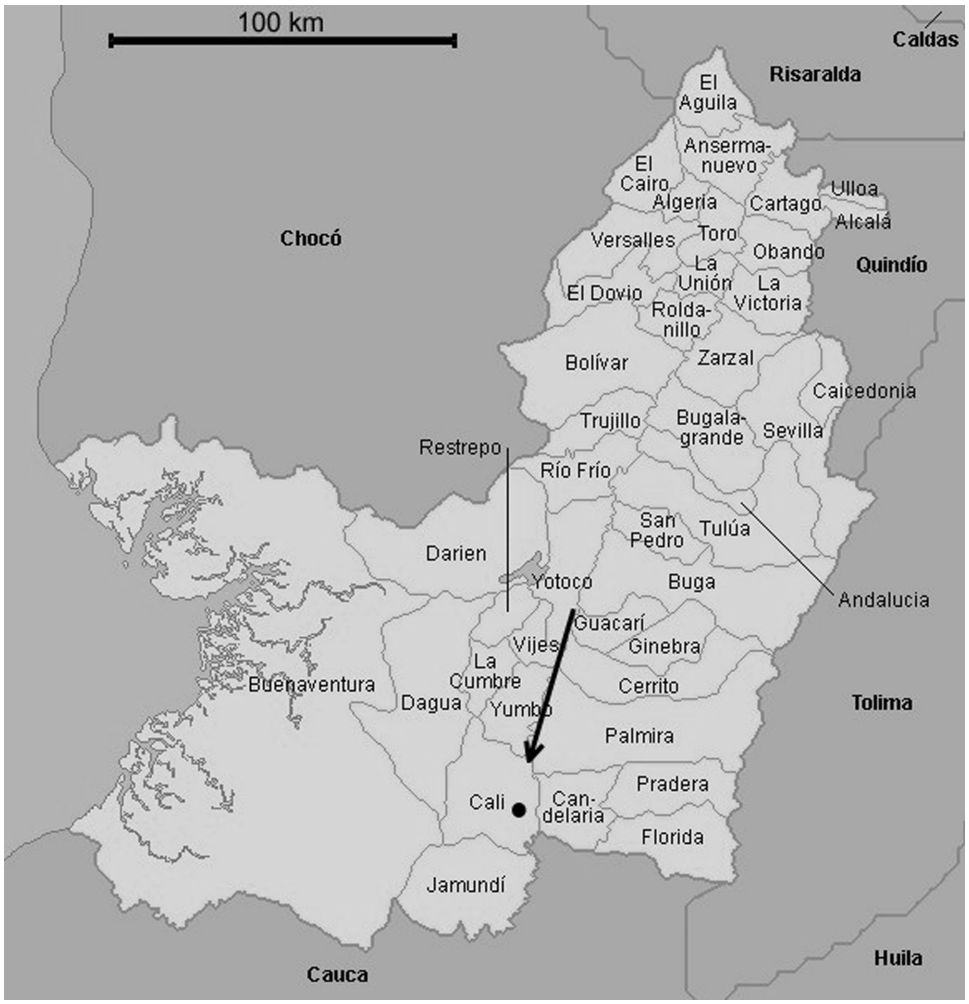

Fig. 2. Map of the Cauca Valley showing a ground projection of the Cali bolide trajectory. A black dot in the region of Cali locates the meteorite strewn field.

events with similar characteristics are clearly noticeable. The first one is found at the HOQC station beginning at 21:34:35 UTC and the other at the SEGC station, 50 seconds later. This means that the hypothetical detection of the bolide's sonic wave front locates the second station 15 km from the first one. The amplitudes are very similar, consistent with the proximity of the two stations to the bolide path.

MINERALOGICAL, PETROLOGICAL, CHEMICAL, AND PHYSICAL PROPERTIES

Analytical Methods and Specimens

Two thin sections were examined in this study: UCLA-1899, prepared from a 20 g stone designated #6 (Connolly et al. 2008), was used for petrographic observations and preliminary electron-microprobe analyses of olivine, pyroxene and kamacite, all done at UCLA. A second thin section prepared by the Smithsonian Institution (unnumbered) from the type specimen derived from the 90 g stone #9 was used for a detailed electron-microprobe study of olivine and pyroxene compositions at the U.S. Geological Survey (USGS).

Because chondrule size-frequency distributions tend to be log normal (e.g., Fig. 1a of Nelson and Rubin [2002]), chondrule apparent diameters were measured in φ units in transmitted light with a calibrated reticle. φ units are defined by the relationship

$$\varphi = -\log_2 d \quad (1)$$

where d is the average apparent diameter of the chondrule in millimeters.

Microprobe analyses for olivine and pyroxene at the USGS were done on a JEOL JXA-8900 using a focused beam with a 15 nA beam current, 15 kV accelerating voltage, and wavelength dispersive spectrometers. Data were calibrated using natural and synthetic silicate and oxide standards and corrected by standard ZAF methods. A total of 93 olivine and 61 low-Ca pyroxene grains were selected at random using an ~10 × 17 grid of points (spacing ~0.6 mm)

covering the thin section; if a grid point fell on a different phase, the analysis was performed on the nearest olivine or pyroxene grain to the original point. Points were also moved slightly if they fell on a crack, inclusion, or within several micrometers of a grain boundary. Preliminary analyses of 20 olivine and 24 low-Ca pyroxene grains were done using similar analytical methods on the JEOL JXA-8200 electron microprobe at UCLA. In addition, 10 randomly selected kamacite grains were analyzed at UCLA using the method of Rubin (1990).

The bulk composition of Cali was determined in two samples (~150 mg each) from ~1.2 g of the interior of stone #6 by wet chemical methods (Llorca et al. 2007). Two independent methods were used for sample preparation: 1) an acid digestion treatment in a sealed Teflon reactor; and 2) alkaline fusion in a zirconium crucible. Analyses were performed by means of inductively coupled plasma mass spectrometry (ICP-MS) and inductively coupled plasma optical emission spectroscopy (ICP-OES).

Three types of physical measurements were made on the Cali specimens: 1) natural and induced thermoluminescence properties were measured in two fragments of stone #6 using apparatus and techniques described in earlier publications (e.g., Benoit et al. 1993a); 2) magnetic susceptibility measurements were carried out at 300 K and 0.5 mT on two samples (128–149 mg) from ~1.2 g of the interior of stone #6; 3) the bulk density and the grain density were determined with a helium pycnometer (ρg, density that excludes pores and voids).

Physical Description

Most of the specimens found were quickly identified as meteorites because they exhibited a prominent fusion crust covering part of their surface (Fig. 1). The interior of those pieces that broke during impact appear granular and dominated by large chondrules. Most of the large pieces were broken, but the small ones are completely fusion crusted.

Petrography

Cali contains well-defined chondrules of all major textural types, ranging from 160 to 2000 μm in apparent diameter. The mean apparent diameter of 65 chondrules in section UCLA-1899 is 1.92 ± 0.71 φ (i.e., 260 +170/–100 μm).

A few cryptocrystalline chondrules and chondrule fragments have a ~60 μm thick bleached zone at their margins, indicative of the parent body's aqueous alteration (Grossman et al. 2000). One barred olivine chondrule 1100 μm in diameter is surrounded by a 100 μm thick igneous rim that is itself enclosed by a 50–150 μm thick rim of metallic Fe-Ni and troilite.

Olivine grains exhibit undulose extinction and contain planar fractures, consistent with shock stage S3 (Stöffler et al. 1991). Several large polycrystalline troilite nodules (900–2800 μm) containing small (~60 μm) patches of metallic Fe-Ni occur. Some metallic Fe-Ni grains contain small equant and elongated grains of metallic Cu (ranging up to 2 × 25 μm) adjacent to small (4–10 μm) irregular grains of troilite. There are rare thin, elongated chromite veinlets within olivine grains; one such veinlet is 0.8 × 26 μm in size.

Table 2. Computed trajectory of the bolide projected on the ground. Note that the fireball was observed in broad daylight, so the computed beginning point is lower than usual.

Beginning point (h = 65 km)		Ending point (h = 17 km)	
Longitude	Latitude	Longitude	Latitude
76.38 ± 0.05°W	3.85 ± 0.05°N	76.44 ± 0.05°W	3.63 ± 0.05°N

Opaque veins, several hundred micrometers in length, composed mainly of troilite and metallic Fe-Ni, occur throughout the meteorite (Fig. 4a). Some opaque assemblages partially surround chondrules (Figs. 4b, 4c); some of these chondrules are transsected by thin opaque veinlets (Fig. 4c).

The meteorite appears to be brecciated. Thin section UCLA-1899 contains four adjacent dark angular clasts (300 to 2000 μm) composed of small (4–15 μm) mafic silicate grains surrounded by thin rinds of feldspathic material, numerous ragged 2–40 μm metal-sulfide assemblages, and relatively coarse (20–350 μm in size) chondrule fragments and isolated olivine and low-Ca pyroxene grains.

Mineral Chemistry

Cali shows a wide range of compositions of low-Ca pyroxene and a relatively narrow distribution of olivine compositions with a few low-FeO outliers (Fig. 5). The mean composition of low-Ca pyroxene grains measured at the USGS is $Fs_{15.8 \pm 6.9}Wo_{1.3 \pm 1,2}$, with a percent mean deviation (PMD) of FeO in pyroxene of 34%. The mean olivine composition is $Fa_{22.5 \pm 2.3}$, with a PMD of FeO in olivine of 4%. Excluding the two low-FeO grains, the mean olivine composition becomes $Fa_{22.8 \pm 0.9}$ with PMD = 2%. For comparison, the mean pyroxene and olivine compositions measured in the preliminary study at UCLA, in which only cores of large grains were analyzed, were $Fs_{12.1 \pm 5.9}Wo_{0.8 \pm 0,8}$ and $Fa_{22.4 \pm 0,3}$, respectively. The mean Co content of kamacite is 0.66 wt%.

Physical Properties

We determined a natural TL value of 34 ± 1 krad for Cali, consistent with an observed fall with a "normal" radiation and thermal history (Benoit et al. 1993b), i.e., similar to the ~95% of falls that have not been within

Table 3.The estimated radiant coordinates and trajectory beginnings (for the fixed beginning height of 65 km). The azimuth is measured from the north toward the east.

Apparent radiant				Beginning point (h = 65 km)	
Azimuth (°)	Elevation (°)	α (°)	δ (°)	Longitude	Latitude
15	62	179 ± 2	31 ± 2	76.38 ± 0.05°W	3.85 ± 0.05°N

Table 4. Computed orbital elements (J2000.0) for the probable range of radiant azimuths and several possible preatmospheric velocities of the fireball.

Velocity (km/s)	a (AU)	e	q (AU)	Q (AU)	ω (°)	Ω (°)	i (°)
12	1.19	0.18	0.977	1.39	137.8	104.349	3.8
15	2.28	0.57	0.988	3.57	157.4	104.343	7.9
18	9.47	0.89	0.987	17.95	159.7	104.341	10.0
Summary	>1	Any	0.98 ± .02	>1	149 ± 11	104.345 ± 0.004	<10

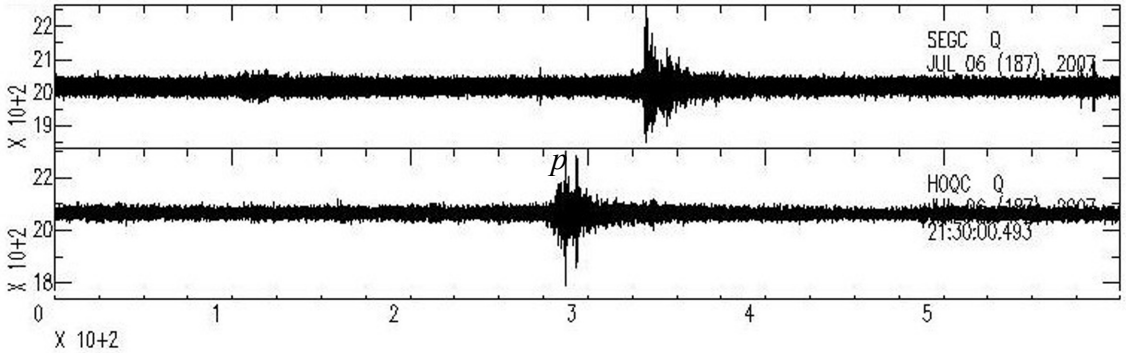

Fig. 3. The signal of the fireball as plotted over a 10 min. interval of seismic velocity recordings at SEGC and HOQC stations (UVC Universidad del Valle, Cali, Colombia) beginning at 21:30:00 UTC.

0.95 AU of the Sun (which would cause a factor of 10–100 lower natural TL; Hasan et al. 1987) and have not recently (within the last 10^5 years) transferred to a near-Earth orbit (like the major ALH 85110 fall and its many paired fragments; Benoit and Sears 1993). These conclusions are consistent with the orbit calculated above from eyewitness observations.

The two samples of Cali we measured for the present study had induced TL values of 1.28 ± 0.18 and 1.64 ± 0.08, relative to Dhajala = 1.

The specific magnetic susceptibility, χ, is log χ (in 10^{-9} m^3 kg^{-1}) = 5.11 ± 0.07.

The bulk density of the Cali meteorite is 3.62 ± 0.10 g·cm^{-3} and the grain density (ρg) determined with a helium pycnometer is 3.74 ± 0.05 g·cm^{-3}. From these values, the porosity of Cali was calculated to be 3.2%.

Bulk Chemistry

The elemental composition that we measured for the Cali meteorite is compiled in Table 5 (mean values and standard deviation). Key measurements for classification purposes include an Fe content of 24.7 wt%, Mg/Si = 0.86, Al/Si = 0.07, and Fe/Si = 1.47.

CLASSIFICATION

Petrologic Type

Induced TL properties relate to the amount and nature of the major luminescence phosphor, which in ordinary chondrites is feldspar. This, in turn, depends mainly on the metamorphic history and thus the petrologic type of the meteorite. Sears et al. (1980) first showed that petrologic types 3, 4, 5 and 6 had TL sensitivity ranges of 0.002 to 1.0, 1.8 to 6.0, 6.0 to 14, and 6.0 to 25, respectively.

While considerable work has been published on the type 3 ordinary chondrites, very little attention has been given to the higher types. Based on existing data, our Cali induced TL measurements of 1.28 and 1.64, relative to Dhajala, suggest that this meteorite is either a very high type 3 (say 3.8 or 3.9) or petrologic type 4. The peak temperature and peak width, i.e., the temperature during readout at which induced TL intensity is at a maximum and the width of the peak at half-maximum, are 192 ± 15 °C and 137 ± 12 °C, for the first sample and 178 ± 4 °C and 139 ± 1 °C for the second sample, which would also be consistent with a high (greater than 3.5) petrologic type.

Other properties indicate that Cali is petrologic type 4 rather than high type 3. These include its moderate degree of

recrystallization, the absence of igneous glass in most chondrules (and presence of turbid glass in a few chondrules), the occurrence of polysynthetically twinned low-Ca clinopyroxene phenocrysts in some porphyritic pyroxene (PP) and porphyritic olivine-pyroxene (POP) chondrules, and relatively homogeneous olivine and heterogeneous low-Ca pyroxene compositions. Using the criteria of Van Schmus and Wood (1967), PMD_{FeO} for olivine is 4%, which is below the 5% minimum value defined for type 3 chondrites. This low value, coupled with the large scatter in pyroxene compositions (PMD_{FeO} for low-Ca pyroxene is 35%) is similar to observations in other type 4 chondrites (Dodd et al. 1967), reflecting slower diffusion of Fe in pyroxene than in olivine during thermal metamorphism.

Chondrite Group

All of the measured chemical, physical, and mineralogical properties of Cali seem to be intermediate between established ranges for the H and L chondrite groups. The bulk Fe content of 24.7 wt% is between the values measured by Kallemeyn et al. (1989) for H chondrites (27.1 wt%) and L chondrites (21.6 wt%), as are the other common siderophile elements and Ir, which average ~0.87 × H and ~1.26 × L. Cali's siderophile abundances are similar to those in the Tieschitz and Bremervörde falls, which have both been classified as intermediate or transitional between the H and L groups (Kallemeyn et al. 1989). Other major and minor elements in Cali are similar to the bulk H and L group values given by Kallemeyn et al. (1989) and Jarosewich (1990), which do not discriminate between the groups.

The measured magnetic susceptibility value for Cali of 5.11 is also intermediate between those of L chondrite falls, 4.87 ± 0.10, and H chondrite falls, 5.31 ± 0.12 (Rochette et al. 2003; Smith et al. 2006). Again, the value in Cali is very similar to those of Tieschitz (4.97) and Bremervörde (4.98) (Rochette et al. 2003).

Magnetic susceptibility and grain density are commonly correlated for meteorite falls because both are intensive variables that vary with iron content (Britt et al. 2003; Consolmagno et al. 2006). The values of magnetic susceptibility and grain density of Cali plot at the edge of the H-chondrite group in a χ versus ρ_g graph for meteorite falls (Consolmagno et al. 2006).

Several mineralogical properties of equilibrated ordinary chondrites (EOCs) can be used to classify these meteorites into individual chondrite groups. Two of the more important parameters are the compositions of olivine and kamacite (Rubin 1990). Cali kamacite is intermediate between the published ranges for H and L chondrites. Rubin (1990) found that the upper limit for H4–6 chondrites is 0.51 wt% Co and the lower bound for L4–6

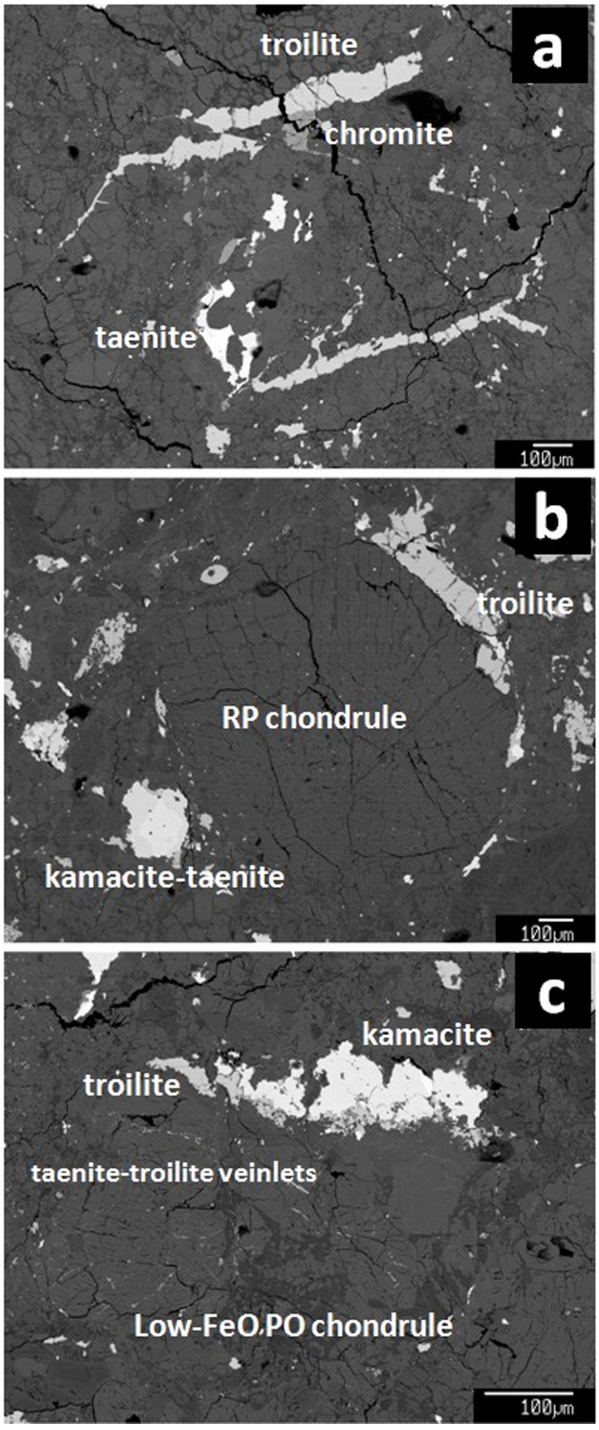

Fig. 4. Backscatter electron images showing opaque assemblages in Cali. a) Subparallel shock veins composed mainly of troilite and taenite. The upper vein has been sheared by an impact event that occurred after the one that initially produced the vein. Minor chromite attached to the vein has also been sheared. b) A radial pyroxene (RP) chondrule partially surrounded by opaque grains. c) A low-FeO (Type I) chondrule transsected by thin veinlets composed mainly of taenite and troilite. At the top of the chondrule there is an irregular, elongated opaque mass (possibly a shock vein) composed of kamacite and troilite.

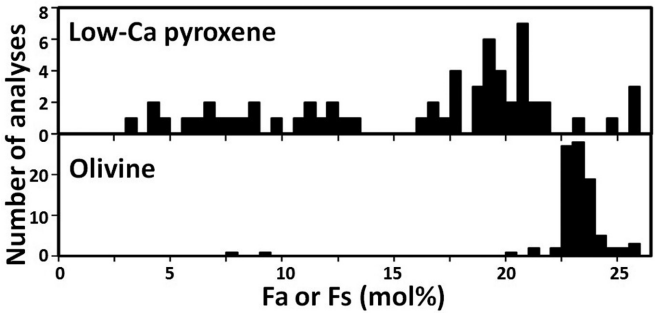

Fig. 5. Histograms of olivine and low-Ca pyroxene compositions in Cali.

chondrites is 0.70 wt% Co. Cali falls in between at 0.66 wt% Co.

The most commonly used parameter for classifying ordinary chondrites into the H, L, and LL groups is the Fa content of olivine. In Fig. 6, we show our data for Cali along with the recommended ranges for each of these groups from Rubin (1990). Because Rubin, like others before him, attempted to define the ranges of groups, his study was based on a fairly small data set (134 samples). Figure 6 also shows for comparison a histogram of 8178 EOC analyses listed in MetBase (Köblitz 2005) that are reported to at least one decimal place (this excludes data measured by imprecise methods).

As was the case for bulk chemical and physical properties, Fig. 6 shows that the composition of olivine in Cali is intermediate between the ranges for H and L chondrites from Rubin (1990). The mean composition of $Fa_{22.5 \pm 2.3}$ is below the recommended lower cutoff of $Fa_{23.0}$ for equilibrated L chondrites and well above the recommended upper cutoff for H chondrites at $Fa_{20.2}$. Even without the two low-Fa olivines shown in Fig. 5, the mean olivine composition is still below the L range.

The comprehensive olivine histogram in Fig. 6 shows a minimum value in the Fa distribution between the H and L peaks at $Fa_{22.0}$, and it is tempting to simply redefine the border between the groups at this point. We note, however, that the low-Fa tail of the L peak cannot be modeled by a Gaussian fit of the peak, which would predict much lower numbers of meteorites in the tails. Although we do not know if a Gaussian curve is really the best model for an asteroidal distribution, we consider it possible that there is another peak buried in this tail. Without a detailed study of all the properties of the chondrites in this range of Fa values, which is beyond the scope of this paper, we are not prepared to recommend changes to the Rubin (1990) range for L chondrites.

Because of the intermediate olivine composition, and with no resolution provided by the bulk chemical or physical properties, the classification of Cali as H or L is problematic. In MetBase (Köblitz 2005), there are about 70 other EOCs with olivine between $Fa_{22.0}$ and $Fa_{23.0}$, and every one of these has been classified as an L chondrite despite the lack of published guidelines for doing so; these are represented by the bars in the histogram just above and below Cali in Fig. 6. The recently described Königsbrück meteorite is also in this Fa range ($Fa_{22.6}$), but was classified as H/L4 (Connolly et al. 2006), similar to literature classifications for the intermediate type 3 ordinary chondrites, Tieschitz and Bremervörde. We note that there are also about two dozen EOCs classified as H/L listed in the Meteoritical Bulletin online database (15 May 2008 version), but in contrast to the situation at the low end of the L distribution, most of these have Fa values that are actually in the H-chondrite range of Rubin (1990), up to ~Fa_{21}.

Clearly, the current classification literature is a bit chaotic, and it is likely that different labs are using different (or poorly defined) criteria. Based on the shape of the H- and L-chondrite peaks in Fig. 6, we do not think that EOCs with olivine in the range $Fa_{20.2}$ to $Fa_{23.0}$ can be confidently classified as L or H chondrites unless there are supporting data (e.g., chemical or isotopic composition, exposure ages) that can lend support to placing them in one of the groups.

Therefore, based on all of our data, and using terminology established for other meteorites with similar properties, we classify Cali as H/L4. We emphasize that the slash indicates uncertainty: it could be either an H chondrite or an L chondrite with properties near the ends of the chemical and mineralogical trends for its group. Alternatively, Cali could be a member of an as yet uncharacterized ordinary chondrite group originating from a different parent asteroid that has mineralogical properties intermediate between those in H and L chondrites; in this case, Cali would be a member of a new, unnamed chondrite group.

CONCLUSIONS

We classify the Cali meteorite as an H/L4 ordinary chondrite breccia. Bulk chemistry reveals that the measured abundances for most elements closely match the values recorded for other ordinary chondrites classified as H/L, including Bremervörde (H/L3.9) and Tieschitz (H/L3.6) (Kallemeyn et al. 1989). Mineralogical and physical properties are intermediate between H and L chondrites. The visual observations made by 20 observers of the daylight bolide (July 6, 2007) have allowed the determination with moderate accuracy of the atmospheric trajectory, radiant, and range of orbital elements of the progenitor meteoroid. Some assumptions of the bolide preatmospheric velocity suggest an origin in the main asteroid belt as in the case of the nine previous meteorites with known orbital elements. Unfortunately, the absence of video recordings capable of an accurate determination of the preatmospheric bolide's velocity makes it impossible to assess the dynamic

Table 5. Elemental abundances in the Cali meteorite.

Element	Unit	Sample preparation	Method	Cali
Na	$mg \cdot g^{-1}$	a.d.	ICP-OES	6.7 ± 0.1
Mg	$mg \cdot g^{-1}$	a.d.	ICP-OES	144 ± 2.0
		a.f.	ICP-OES	148 ± 2.6
Al	$mg \cdot g^{-1}$	a.d.	ICP-OES	11.7 ± 0.3
		a.f.	ICP-OES	11.5 ± 0.2
Si	$mg \cdot g^{-1}$	a.f.	ICP-OES	168.3 ± 3.8
P	$mg \cdot g^{-1}$	a.d.	ICP-OES	1.0 ± 0.1
S	$mg \cdot g^{-1}$	a.d.	ICP-OES	20.6 ± 0.8
K	$\mu g \cdot g^{-1}$	a.d.	ICP-OES	786 ± 90
Ca	$mg \cdot g^{-1}$	a.d.	ICP-OES	12.7 ± 0.2
		a.f.	ICP-OES	12.8 ± 0.2
Sc	$\mu g \cdot g^{-1}$	a.d.	ICP-MS	8.1 ± 0.4
Ti	$\mu g \cdot g^{-1}$	a.d.	ICP-OES	716 ± 5
Cr	$mg \cdot g^{-1}$	a.f.	ICP-OES	3.7 ± 0.1
Mn	$mg \cdot g^{-1}$	a.d.	ICP-OES	2.4 ± 0.1
Fe	$mg \cdot g^{-1}$	a.d.	ICP-OES	247 ± 7
		a.f.	ICP-OES	244 ± 9
Co	$\mu g \cdot g^{-1}$	a.d.	ICP-OES	730 ± 15
Ni	$mg \cdot g^{-1}$	a.d.	ICP-OES	14.5 ± 0.2
Cu	$\mu g \cdot g^{-1}$	a.d.	ICP-MS	115 ± 1.0
Zn	$\mu g \cdot g^{-1}$	a.d.	ICP-MS	48 ± 1.0
Ga	$\mu g \cdot g^{-1}$	a.d.	ICP-MS	5.7 ± 0.5
Os	$\mu g \cdot g^{-1}$	a.d.	ICP-MS	0.71 ± 0.05
Ir	$\mu g \cdot g^{-1}$	a.d.	ICP-MS	0.68 ± 0.02

a.d. = acid digestion; a.f. = alkaline fusion.

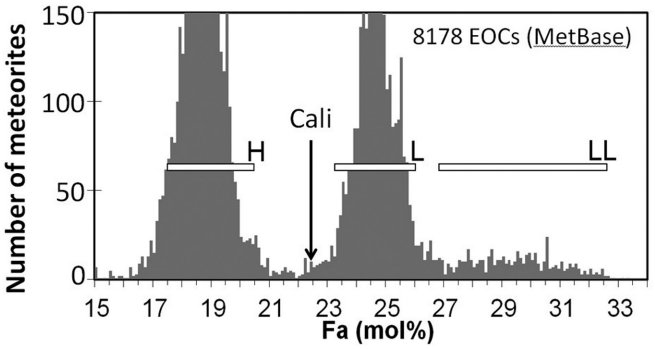

Fig. 6. Histogram showing the average Fa content of olivine (mol%) in Cali and 8178 type 4–6 ordinary chondrites from the literature. The recommended ranges for H, L, and LL chondrites (horizontal bars) are from Rubin (1990). Histogram data were selected from MetBase (Koblitz 2005), and represent all analyses that are reported with at least one decimal place (this excludes most data measured by imprecise methods). Bars have been truncated at N = 150, but would rise to N = 364 and 201 in the sharp H and L peaks, respectively.

mechanism that put this meteoroid into an Earth-crossing orbit. The thermoluminescence value of 34 ± 1 krad is also consistent with an observed fall with a "normal" radiation and thermal history that originated from a progenitor meteoroid that has not been within 0.95 AU of the Sun and has not recently (within the last 10^5 years) been transferred to a near-Earth orbit. These conclusions are consistent with the range of orbital elements calculated from eyewitness observations.

Acknowledgments—We thank the efforts made by ASAFI and EAC members who participated in the trajectory reconstruction and meteorite recovery: Julieta Arboleda, Yamileth Carvajal, Diego Castaño, Diana Castaño, Luz M. Duque, Luz Ángela Espinoza, Jair González, Juan C. Mejía, Julio Monsalvo, Monique Monsalvo, Fabricio Noguera, and Guillermo Vega. We thank Diana Mendoza (OSSO-Universidad del Valle) for kindly providing us with the seismic velocity recordings of the bolide. We also express our gratitude to all eyewitnesses who reported trajectory data: Teresa Arce, Martín Caicedo, Hernando Ceballos, Janet Collazos, Martín Collazos, Alfredo Chávez, Nelson E. Escobar, Martha L. García, Juan M. Guzmán, Alberto Hernao, Omar Hernández, Andrés F. López, Iván M. López, Fabián Orozco, John J. Orozco, Luís Rivas Puente, John J. Sánchez, Julián Stevens, Lisa M. Téllez, H. Vivas. We are grateful to Gustavo Noguera and Yolanda Polanco for providing meteorite specimens for study. Prof. Jorge F. Estela Uribe (Pontificia Universidad Javeriana de Cali) supported the meteorite recovery and sending of samples for study. Meteorite location information and the specimen used for petrographic analysis were generously provided by Mike Farmer. This work was partially supported by NASA Cosmochemistry grants NNH05AB65I to JNG and NNG06GF95G to AER and NASA Discovery Data Analysis grant NNX08G17G to DWGS. JMTR also thanks CSIC for a JAE-Doc research contract.

Editorial Handling—Dr. Adrian Brearley

REFERENCES

Benoit P. H., Jull A. J. T., McKeever S. W. S., and Sears D. W. G. 1993a. The natural thermoluminescence of meteorites VI: Carbon-14, thermoluminescence and the terrestrial ages of meteorites. *Meteoritics* 28:196–203.

Benoit P. H., Sears D. W. G., and McKeever S. W. S. 1993b. Natural thermoluminescence and terrestrial ages of meteorites from a variety of temperature regimes. *Radiation Detection Dosimetry* 47:699–674.

Benoit P. H. and Sears D. W. G. 1994. A recent meteorite fall in Antarctic with an unusual orbital history. *Earth and Planetary Science Letters* 120:463–471.

Britt D. T. and Consolmagno G. J. 2003. Stony meteorite porosities and densities: A review of the data through 2001. *Meteoritics & Planetary Science* 38:1161–1180.

Ceplecha Z. 1987. Geometric, dynamic, orbital and photometric data on meteoroids from photographic fireball networks. *Bulletin of Astronomical Institute of Czechoslovakia* 38:222–234.

Connolly H. C. Jr., Zipfel J., Grossman J. N., Folco L., Smith C., Jones R. H., Righter K., Zolensky M., Russell S. S., Benedix G. K., Yamaguchi A., and Cohen B. 2006. The Meteoritical Bulletin, No. 90, 2006 September. *Meteoritics & Planetary Science* 41:1383–1418.

Connolly H. C. Jr., Smith C., Benedix G. K., Folco L., Righter K., Zipfel J., Yamaguchi A., Chennaoui Aoudjehane H. 2008. Meteoritical Bulletin, No. 93. *Meteoritics & Planetary Science* 43:571–632.

Consolmagno G. J., Macke R. J., Rochette P., Britt D. T., and Gattacceca J. 2006. Density, magnetic susceptibility, and the characterization of ordinary chondrite falls and showers. *Meteoritics & Planetary Science* 41:331–342.

Docobo J. A., Trigo-Rodríguez J. M., Borovička J., Tamazian V. S., Fernández V. A., and Llorca J. 2007. March 1, 2005 daylight fireball over Galicia (NW of Spain) and Minho (N. Portugal). *Earth Moon and Planets* 102:537–542.

Dodd R. T., Van Schmus W. R., and Koffman D. M. 1967. A survey of the unequilibrated ordinary chondrites. *Geochimica et Cosmochimica Acta* 31:921–951.

Grossman J. N., Alexander C. M. O.'D., Wang J., and Brearley A. J. 2000. Bleached chondrules; evidence for widespread aqueous processes on the parent asteroids of ordinary chondrites. *Meteoritics & Planetary Science* 35:467–486.

Hasan F. A., Haq M., and Sears D. W. G. 1987. Natural thermoluminescence levels in meteorites, I: 23 meteorites of known Al-26 content. Proceedings, 17th Lunar and Planetary Science Conference, Part 2. *Journal of Geophysical Research* 92: E703–E709.

Jarosewich E. 1990. Chemical analyses of meteorites: A compilation of stony and iron meteorite analyses. *Meteoritics* 25:323–337.

Kallemeyn G. W., Rubin A. E., Wang D. Y., and Wasson T. W. 1989. Ordinary chondrites: Bulk compositions, classification, lithophile-element fractionations, and composition-petrographic type relationships. *Geochimica et Cosmochimica Acta* 53:2747–2767.

Koblitz J. 2005. MetBase version 7.1 for Windows. CD-ROM.

Llorca J., Gich M., and Molins E. 2007. The Villalbeto de la Peña meteorite fall: III. Bulk chemistry, porosity, magnetic properties, Fe^{57} Mössbauer spectroscopy, and Raman spectroscopy. *Meteoritics & Planetary Science* 42:A177–A182.

Nelson V. E. and Rubin A. E. 2002. Size-frequency distributions of chondrules and chondrule fragments in LL3 chondrites: Implications for parent-body fragmentation of chondrules. *Meteoritics & Planetary Science* 37:1361–1376.

Pujol J., Rydelek P., and Ishihara J. 2006. Analytical and graphical determination of the trajectory of a fireball using seismic data. *Planetry and Space Science* 54:78–86.

Rochette P., Sagnotti L., Bourot-Denise M., Consolmagno G., Folco L., Gattacceca J., Osete M. L., and Pesonen L. 2003. Magnetic classification of stony meteorites. 1. Ordinary chondrites. *Meteoritics & Planetary Science*:251–268.

Rubin A. E. 1990. Kamacite and olivine in ordinary chondrites: Intergroup and intragroup relationships. *Geochimica et Cosmochimica Acta* 54:1217–1232.

Sears D. W., Grossman J. N., Melcher C. L., Ross L. M., and Mills A. A. 1980. Measuring the metamorphic history of unequilibrated ordinary chondrites. *Nature* 287:791–795.

Smith D. L., Ernst R. E., Samson C., and Herd R. 2006. Stony meteorite characterization by non-destructive measurement of magnetic properties. *Meteoritics & Planetary Science* 41:355–373.

Stöffler D., Keil K., and Scott E. R. D. 1991. Shock metamorphism of ordinary chondrites. *Geochimica et Cosmochimica Acta* 55. 3845–3867.

Trigo-Rodríguez J. M., Borovička J., Spurný P., Ortiz J. L., Docobo J. A., Castro-Tirado A. J., and Llorca J. 2006. The Villalbeto de la Peña meteorite fall: II. Determination of the atmospheric trajectory and orbit. *Meteoritics & Planetary Science* 41:505–517.

Van Schmus W. R. and Wood J. A. 1967. A chemical-petrologic classification for the chondritic meteorites. *Geochimica et Cosmochimica Acta* 31:747–765.